ELSEVIER

Diamond and Related Materials 4 (1995) 661–665

DIAMOND AND RELATED MATERIALS

I/V characteristics of epitaxial Schottky Au barrier diode on p^+ diamond substrate

A. Vescan[a], W. Ebert[a], T. Borst[b], E. Kohn[a]

[a]*Department of Electron Devices and Circuits, University of Ulm, 89069 Ulm, Germany*
[b]*Department of Solid State Physics, University of Ulm, 89069 Ulm, Germany*

Abstract

Epitaxial p-type Schottky barrier diodes on synthetic p^+ substrates were analysed in terms of their reverse I/V characteristics. A new electronic model was developed to describe the excess leakage current generally observed in epitaxial diodes. This current is attributed to homogeneously distributed defects, acting only on a small fraction of the diode surface area, bypassing the Schottky barrier contact. Passivation experiments are reported to reduce their density.

Keywords: Diamond Schottky diode; Defect model; Passivation

1. Introduction

Schottky diodes on p-type diamond show a barrier height of $\Phi_B > 1.5$ eV and a low ideality factor ($n = 1.1$), thus making them attractive for high temperature application. However, at low temperature (room temperature), injection mechanisms other than thermionic emission become apparent and contribute to the current transport. Therefore, although the forward I/V characteristics are widely in agreement with thermionic emission, the reverse characteristics are less clear. Theoretically, the high barrier should result in immeasurable low reverse current levels and high breakdown voltages. Indeed, on natural diamond, such a behaviour is observed [1–3]. However, technically relevant diodes on epitaxial layers show high reverse currents, which are thermally activated and do not saturate at high reverse bias [4–9].

2. Experimental details

The diodes used in this investigation (Fig. 1) were fabricated on commercially available, 1 mm thick, [100]-oriented synthetic p^+ diamond substrates (Sumicrystal®). These p^+-doped substrates contain approximately 100 ppm boron and exhibit a conductivity of the order of 10 Ω cm at room temperature. X-Ray analysis shows a clear [100] orientation and a slightly larger lattice constant than undoped material ($\Delta a/a \approx 10^{-4}$). The surface finish is mirror like. However, no information on the defect density is available from the manufacturer, and no defect analysis has been attempted. Prior to epitaxy, the substrates were treated by a super-polish resulting in a surface roughness on the angstrom scale [10].

Two homoepitaxial layers grown by 2.45 GHz microwave plasma CVD in a quartz reactor were used in this investigation. The samples were plasma pre-etched in H_2 for 5 min and grown in a mixture of CH_4 (2%) and H_2 at a total gas pressure of 40 mbar and a flow rate of 50 standard cubic centimetres per minute (sccm). The substrate temperature was held at 800 °C. Boron doping was achieved by controlled evaporation of B_2O_3.

The boron doping concentrations of the active epitaxial layers (extracted by C/V analysis) and the thicknesses

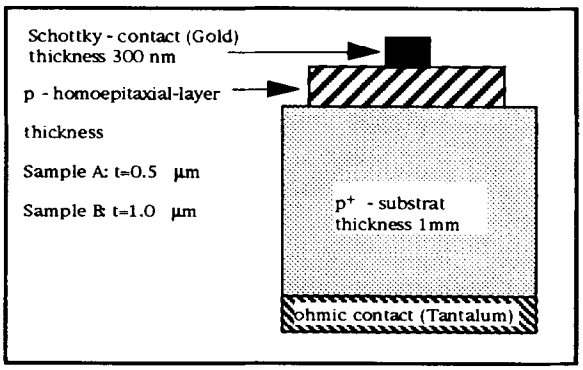

Fig. 1. Structure of the p/p^+ Schottky diodes.

SSDI 0925-9635(94)05237-9

of the samples were as follows: (A) $N_A = 1.1 \times 10^{17}$ cm^{-3}, $t = 0.50$ μm; (B) $N_A = 1.0 \times 10^{17}$ cm^{-3}, $t = 1.00$ μm.

After deposition, the epitaxial layers were cleaned in a saturated solution of CrO_3 in H_2SO_4 at 160 °C, followed by boiling in acetone, methanol and isopropanol and rinsing in deionized water. The Schottky contact metal (Au) was deposited by r.f. sputtering.

Circular contacts with areas between 8×10^{-5} cm^2 and 5×10^{-4} cm^2 were formed by standard lithography and wet chemical etching of the Au layer.

Large area ohmic contacts were made to the reverse side of the p^+ substrates by alloying sputtered Ta at 900 °C in dry argon.

The I/V measurements were performed with an HP4145B parameter analyser in the temperature range between room temperature and 400 °C.

3. Results and discussion

Figs. 2 and 3 show the I/V characteristics of typical diodes on layer configurations A and B respectively. Although only a limited number of diodes were possible on the 3 mm × 3 mm substrate surface area, the diode characteristics did not vary qualitatively. No significant differences, which could be attributed to the different layer thicknesses, were apparent.

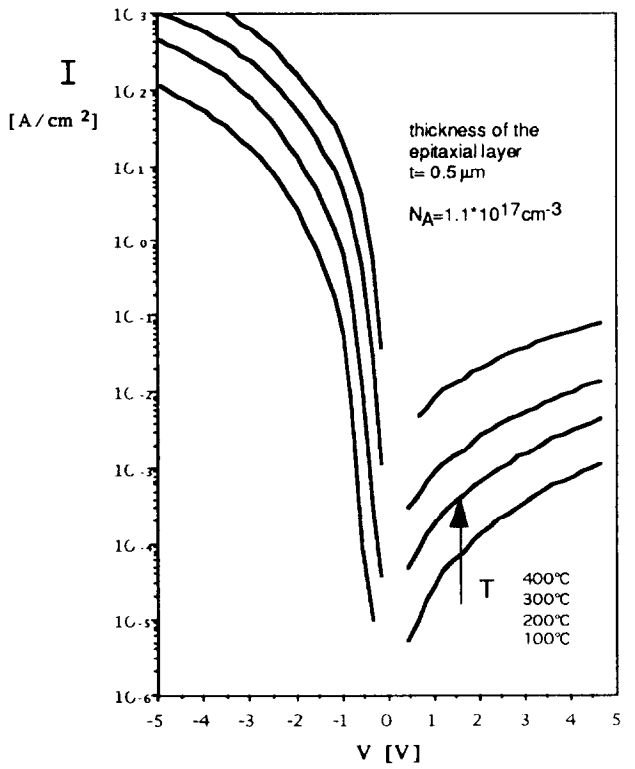

Fig. 2. I/V characteristics of sample A.

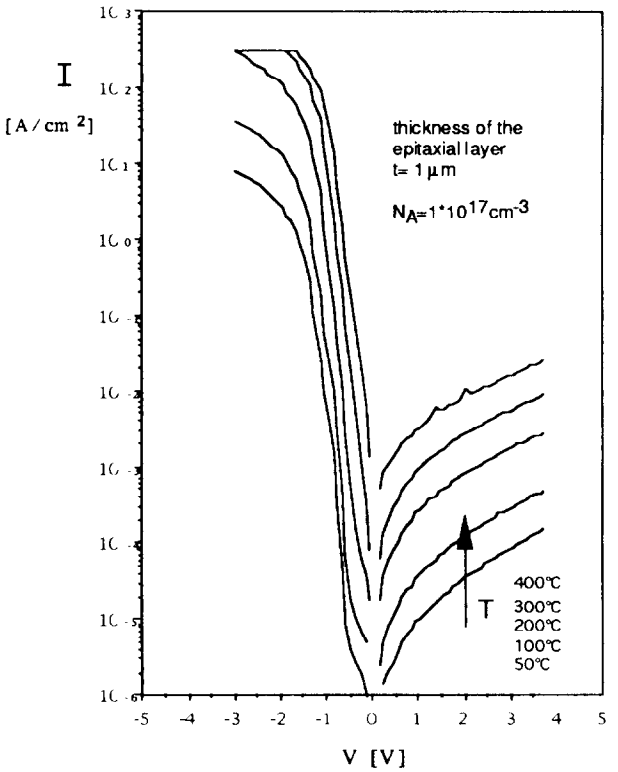

Fig. 3. I/V characteristics of sample B.

3.1. Forward characteristics

At low forward bias, the Schottky diodes show an exponential increase in current over 3–4 orders of magnitude. The lowest observed ideality factor is $1.1 < n < 1.3$ at 400 °C. The I/V Schottky barrier height, extracted from the high temperature part of the characteristics (and thus low ideality factor), is $\Phi_{B(I/V)} \approx 1.5$ eV. From reverse bias C/V measurements, a barrier height of $\Phi_{B(C/V)} \approx 1.7$ eV is extrapolated, which is nearly independent of temperature [4]. The ideality factor increases with decreasing temperature. Thus current paths other than thermionic emission become apparent. This may point towards small area defects contributing to the excess current flow, leading to a reduced effective I/V barrier height.

3.2. Reverse characteristics and defect model

The reverse current levels of the samples are several orders of magnitude (approximately 10^8) above the theoretical limit even when image force lowering is taken into account [10]. A weak exponential voltage dependence and strong temperature dependence are observed.

Possible origins for this excess leakage current are as follows: (a) field-induced barrier lowering and image force barrier lowering; (b) carrier generation in the space charge region; (c) fringing effects at the circumflex; (d)

lateral surface conductivity; (e) tunnelling through defects.

Since the reverse current is proportional to the surface area, fringing effects and lateral surface conductivity have been excluded [3]. The strong thermal activation of the reverse current indicates that tunnelling or thermionic field emission can also be excluded. Carrier generation in the space charge region will lead to an $I/V \propto \sqrt{U}$ dependence and the reverse current will saturate at high bias levels. Since the observed I/V curves show an exponential dependence, carrier generation in the space charge region cannot be the origin of the excess leakage current.

An excess current due to field-induced Schottky barrier lowering would fit both the exponential I/V characteristic and the temperature activation, but is not consistent with the doping concentration of the epitaxial layers and the barrier height of the Schottky contact. This can be seen from the analysis below.

The thermionic emission current density across a Schottky barrier under reverse bias is given by [11]

$$J_R = A^* T^2 \exp\left(-\frac{q\Phi_{B0}}{kT}\right)\exp\left(+\frac{q\sqrt{qE/(4\pi\varepsilon_s)}}{kT}\right) \quad (1)$$

where

$$E = \sqrt{\frac{2qN_A}{\varepsilon_s}\left(V + V_{bi} - \frac{kT}{q}\right)}$$

with the notation used in Ref. [11].

It can be seen that the effective barrier height now becomes bias dependent, and decreases roughly with the fourth root of the bias (V). At higher voltage ($V \gg V_{bi} - kT/q$), Eq. (1) may be converted to

$$\frac{kT}{q}\ln\left(\frac{J_R}{T^2}\right) \cong \frac{kT}{q}\ln(A^*) - \Phi_{B0} + \frac{\sqrt[4]{N_A}}{4.5\times 10^{-6}} \cdot \sqrt[4]{V} \quad (2)$$

Thus in a semi-logarithmic presentation $\ln(J_R/T^2)$ needs to yield straight lines vs. $V^{1/4}$. This is indeed the case as demonstrated with sample A in Fig. 4. However, the extracted doping concentration is $N_{Adef} = 1.5 \times 10^{19}\ \mathrm{cm}^{-3}$, and approximately two orders of magnitude above that extracted from the C/V measurement.

The zero field barrier height can be extracted by extrapolating to $V \to 0$ and by plotting the quantity $[kT/q(\ln A^*) - \Phi_{B0def}]$ vs. T. It yields $\Phi_{B0def} = 0.5$ eV (Fig. 5). Again, this is not consistent with the value extracted from the I/V and C/V Schottky barrier characteristics.

This analysis has also been applied to sample B and similar model data related to the defects were obtained: $5 \times 10^{18}\ \mathrm{cm}^{-3} < N_{Adef} < 5 \times 10^{19}\ \mathrm{cm}^{-3}$ and $0.4\ \mathrm{eV} < \Phi_{B0def} < 0.55$ eV.

Thus a new model is proposed in which the contact

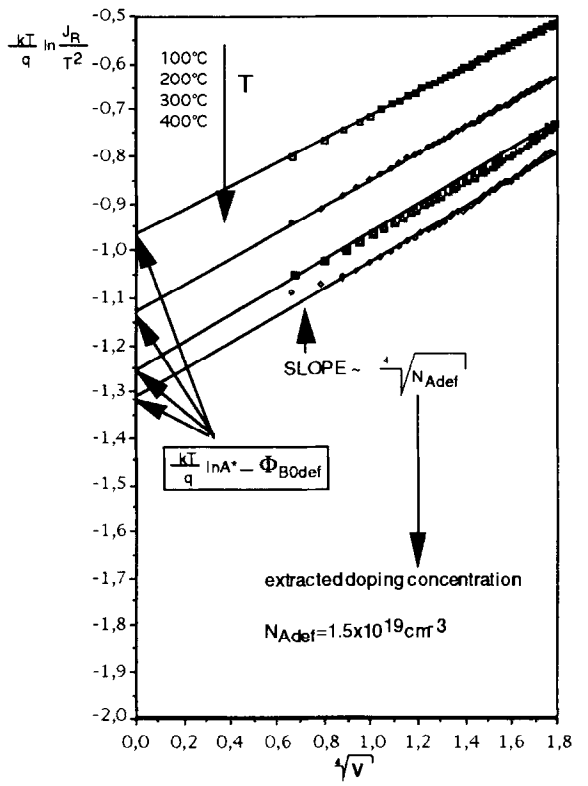

Fig. 4. Plot of Eq. (2) (sample A).

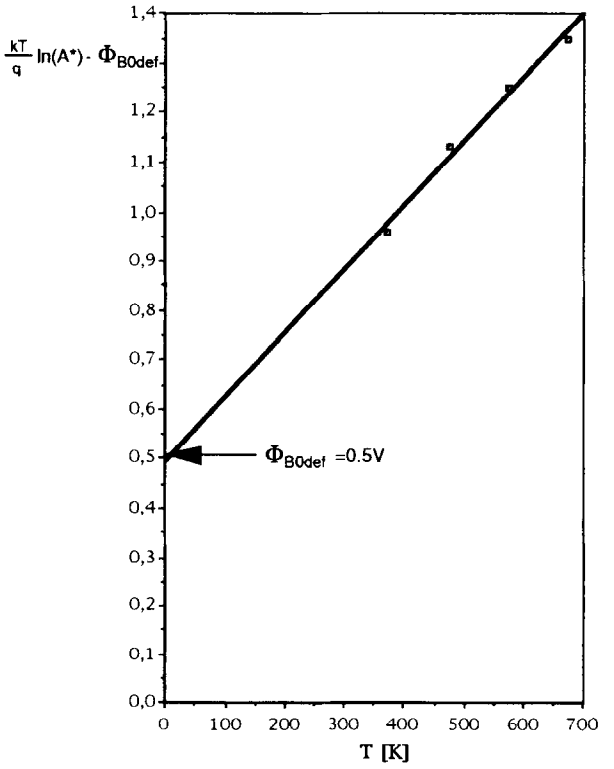

Fig. 5. Extraction of the zero field barrier height.

is divided between the Schottky barrier contact area, which represents the major part of the surface, and a small defect controlled area generating the excess current. These defects are homogeneously distributed across the surface (since the current is proportional to the surface area) and act electronically as highly doped, low barrier height contacts. They also need to be connected through the entire space charge layer in order to contact the neutral region.

However, this electronic model cannot reveal the chemical nature of the defects. It may be speculated that the results are linked to native defects which are H passivated during growth. In this case, it may be possible to passivate these defects near the surface by an O plasma treatment prior to contact metal deposition.

3.3. Defect passivation experiments

Initial passivation experiments were undertaken on sample B. After removing the Schottky metallization by wet chemical etching in aqua regia, the substrate was cleaned in a saturated solution of CrO_3 in H_2SO_4 at 160 °C, followed by boiling in acetone, methanol and isopropanol and rinsing with deionized water. Then, prior to Au Schottky contact deposition, the surface of the epitaxial layer was exposed to an Ar/O plasma (partial pressure 150 mTorr Ar and 150 mTorr O_2; power 10 W). After 2 min, the oxygen supply was interrupted and the sample was exposed to 150 mTorr Ar plasma for a further 3 min.

The result is shown in Fig. 6. In comparison with Fig. 3, the leakage current is reduced below the resolution limit (10 pA). However, the exponential temperature-activated nature still seems to be present. The reduction in value can therefore be translated into a reduction in defect density. Thus the plasma treatment has indeed acted to passivate a substantial number of defect centres.

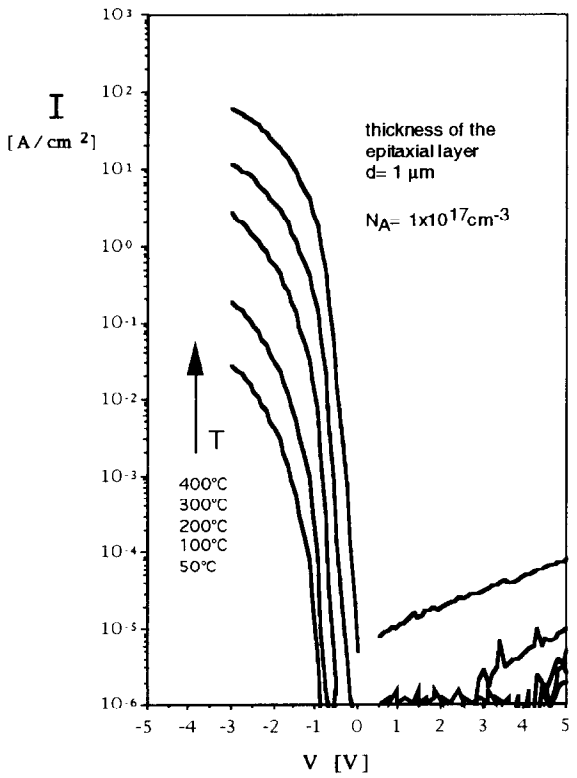

Fig. 6. I/V characteristics of sample B with plasma treatment.

4. Conclusions

Epitaxial p-type Schottky barrier diodes on synthetic p^+ substrates were analysed in terms of their reverse I/V characteristics. A new electronic model was developed to describe the excess leakage current generally observed in epitaxial diodes. This current is attributed to homogeneously distributed defects, acting only on a small fraction of the diode surface area, bypassing the Schottky barrier contact. This new model, in which the defects are described by a high effective doping concentration and a low barrier height, can only be regarded as a first attempt and certainly needs refinement. The high effective doping concentration allows only a thin space charge layer to develop. Thus it may also be interpreted as interfacial charge. The fact that the defects have to contact the neutral region may indicate that they represent pipes reaching through the entire epitaxial layer.

Initial passivation experiments indicate that the electronic defect description may be linked to native defects generated during growth. The reverse current levels have been reduced by three orders of magnitude. However, it seems that the defect nature of the remaining current is preserved. An exponential increase with reverse bias and thermal activation are still present. The reduction in defect density seems critical to obtain diodes which can operate at high reverse bias and high temperature.

Acknowledgments

The authors gratefully acknowledge financial support by the Deutsche Forschungsgemeinschaft (DFG) carried out under the auspices of the trinational "D-A-CH" cooperation of Germany, Austria and Switzerland on the "Synthesis of Superhard Materials". Further support was provided by the State of Baden-Württemberg.

References

[1] M.W. Geis, N.N. Efremow and J.A. von Windheim, *Appl. Phys. Lett.*, *63* (7) (1993) 952–954.

[2] T.P. Humphreys, J.V. LaBrasca, R.J. Nemanich, K. Das and J.B. Posthill, *Jpn. J. Appl. Phys., 30* (1991) L1409.
[3] W. Ebert, unpublished results.
[4] W. Ebert, A. Vescan, T. Borst, O. Weis and E. Kohn, Diamond Film Semiconductors, *SPIE J., 2151* (1994) 83.
[5] W. Ebert, A. Vecan, T. Borst and E. Kohn, *IEEE Electron Device Lett., 15* (1994).
[6] K. Kobashi, K. Nishimura, K. Miyata, R. Nakamura, H. Koyama, K. Saito and D.L. Dreifus, *2nd Int. Conf. on the Application of Diamond Films and Related Materials, Tokyo, 1993*, pp. 35–42.
[7] H. Shiomi, Y. Nishibayashi and N. Fujimori, *Jpn. J. Appl. Phys., 29* (1990) L2163–L2164.
[8] H. Shiomi, K. Tanabe, Y. Nishibayashi and N. Fujimori, *Jpn. J. Appl. Phys., 29* (1990) 34–40.
[9] H. Shiomi, H. Nakahata, T. Imai, Y. Nishibayashi and N. Fujimori, *Jpn. J. Appl. Phys., 28* (5) (1989) 758–762.
[10] P.C. Münzinger and O. Weis, paper presented at *Diamond Films '94, Il Ciocco, September 1994.*
[11] S.M. Sze, *Physics of Semiconductor Devices*, Wiley, New York, 1981, p. 281.